III–E Synthesis and Characterization of Metal Clusters

Recently, metal clusters consisted of several tens or several hundreds of metal atoms have gained much attention as new nano-scaled materials because their properties are significantly different from the corresponding bulk and behave in a size-dependent manner. To exploit a synthetic method of metal clusters while controlling their size in an atomic level is a challenging task which will help us to understand the size-dependent properties of the clusters and open up many possibilities for the wide range of applications. We have addressed the issue by adopting the following approaches: 1) Chemical synthesis of the clusters in the presence of molecular capsules, which work as templates and stabilizers for the clusters and 2) characterization of the clusters by mass spectrometry. Our goal is to reveal the origin of the size-specific chemical reactions occurring on the surface of metal clusters.

III-E-1 Development of Mass Spectrometer for Metal Clusters Dispersed in Liquid Phase

NEGISHI, Yuichi; TSUKUDA, Tatsuya

Mass spectrometry is a powerful diagnostics for the metal clusters because it provides useful information complementary to that obtained from the conventional characterization by TEM; the cluster size and composition can, in principle, be characterized in an atomic resolution. We have constructed an apparatus consisting of electrospray ionization (ESI) source and time-of-flight (TOF) mass spectrometer with a reflectron as shown in Figure 1. Liquid sample containing the metal clusters is pumped through a fused silica capillary, whose end is supported in a stainless steel needle. Charged aerosol droplets are electrosprayed by means of an electrical potential between the needle tip and a counter electrode (+3–5 kV). The cluster ions contained in the droplets are evaporated into the gas phase and further desolvated by passing through a heated capillary. A portion of the ion flow is skimmed and introduced into the acceleration region of the TOF mass spectrometer. Then, the ions are extracted in the direction perpendicular to the initial beam by applying a pulsed voltage of ~15 kV to a set of grids. The ions are stirred by several sets of ion optics and detected by either a microchannel plate (MCP) detector located at the end of the flight path of ~3.2 m (low-resolution mode) or another MCP detector with a center hole after reflected by the coaxial reflectron (high-resolution mode). Figure 2 shows a typical ESI mass spectrum of tetra-*n*-octylammonium bromide obtained in the high-resolution mode.

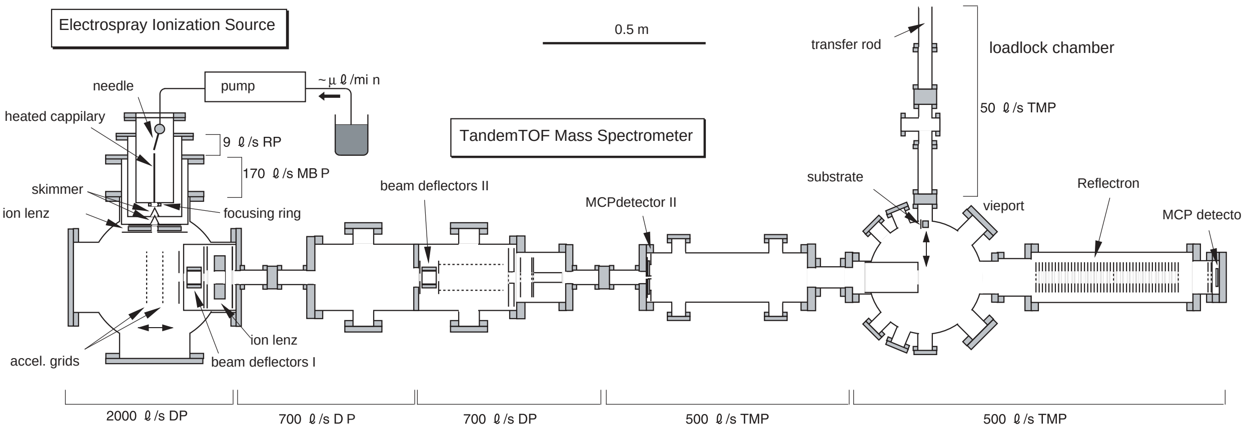

Figure 1. Schematic diagram of the experimental apparatus.

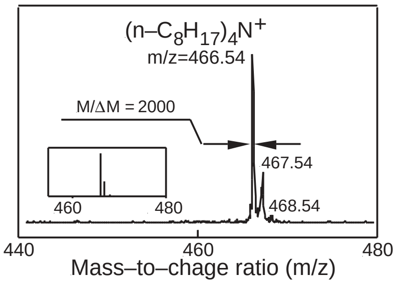

Figure 2. The positive-ion ESI mass spectrum of tetra-*n*-octylammonium bromide run in a methanol mobile phase. Inset shows the isotopic distribution of $(n\text{-}C_8H_{17})_4N^+$ calculated from the natural abundance. Mass resolution of $m/\Delta m$ ~ 2000 is routinely achieved in the high-resolution mode.

III-E-2 Mass Spectroscopic Characterization of Transition Metal Clusters Encapsulated by PAMAM Dendrimers

NEGISHI, Yuichi; TSUKUDA, Tatsuya

Synthesis of metal nanoclusters using dendrimers as “nanotemplates” has been one of the most exciting topics in recent cluster chemistry.$^{1)}$ The dendrimers are hyper-branched polymers, which are almost spherical in shape, sterically crowded on the exterior, and somewhat hollow on the interior. A strategy proposed for preparation of the dendrimer-encapsulated nanoparticles is rather simple:$^{1)}$ Introduction of metal ions into the internal cavity of dendrimers followed by chemical reduction of the metal ions.

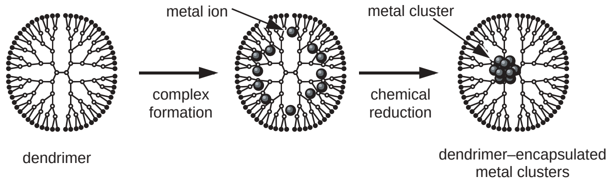

We have followed the synthetic procedures by ESI mass spectrometry. Figure 1A shows ESI mass spectra of OH-terminated poly(amido)amine dendrimers with a third generation (G3-OH). A series of prominent peaks discernible in Figure 1A are assigned to the multiply charged molecular ions of G3-OH with the ideal structure. Mass peaks interspersed between them are due to the G3-OH molecules with missing arms, which are present as contamination in the sample. Figure 1B shows mass spectrum of the complexes of G3-OH and silver ions, which are prepared by mixing 16-fold molar excess of $AgNO_3$. Clusters containing up to 10 Ag ions are recognizable whereas the larger clusters are not because of overlapping of the mass peaks due to the heterogeneity of the G3-OH sample. The chemical reduction of these complexes by $NaBH_4$ or hydrazine results in the formation of Ag clusters stabilized by G3-OH. The ESI spectrum obtained for the clusters is essentially the same with that of free G3-OH (Figure 1C). This observation suggests that the Ag clusters are passivated weakly by several G3-OH which are easily removed during the ES processes. It is conceivable that the aggregation of Ag(0) atoms proceeds outside the dendrimer because of low density of G3-OH surface and/or low partition coefficient of the Ag ions. Following studies are now underway in our group: 1) Purification of the dendrimers by gel permeation chromatography and 2) synthesis of nanoclusters by using dendrimers with higher generations having more dense surfaces.

Reference

1) R. M. Crooks *et al.*, *Topics in Current Chemistry* **212**, 81 (2001) and references therein.

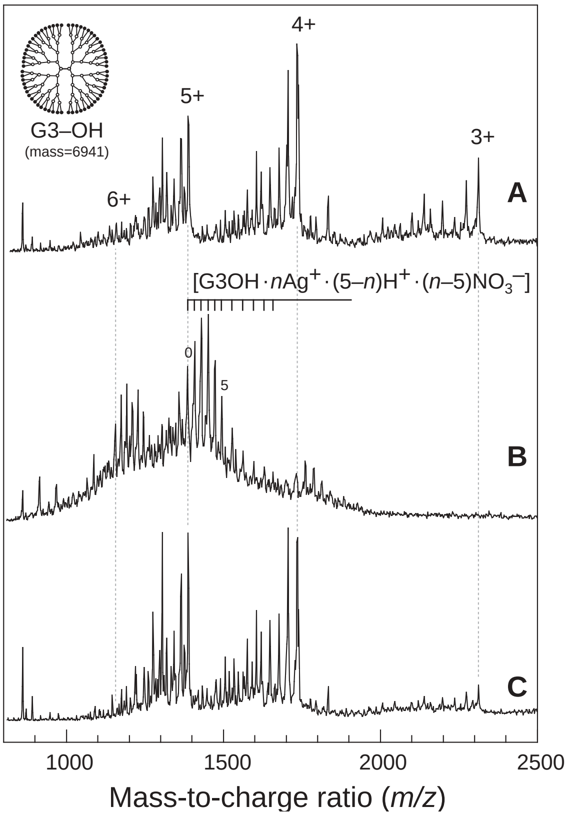

Figure 1. The ESI mass spectra of A) G3-OH PAMAM dendrimers, B) complexes between G3-OH and silver ions, C) silver clusters stabilized by G3-OH.

III-F Geometric and Electronic Structures of Negatively-Charged Molecular Clusters

The geometric and electronic structures of negatively-charged molecular clusters are among the most fundamental issues in cluster science: How do the molecular aggregates trap an excess electron and how do the structures evolve with cluster size? Among the systems studied so far, negatively-charged clusters of carbon dioxide, $(CO_2)_n^-$, have been a prototype system to address these issues. Some intriguing phenomena have been observed in the previous photoelectron spectroscopic studies of $(CO_2)_n^-$ (*Chem. Phys. Lett.* **268**, 429 (1997)): 1) Existence of distinct isomers having different anionic cores of CO_2^- and $C_2O_4^-$ (“electronic isomers”), 2) switching of the anionic core from CO_2^- to $C_2O_4^-$ and vice versa at $n = 7$ and 14, respectively (“core switching”), 3) spontaneous interconversion between $CO_2^- \cdot (CO_2)_5 \rightleftarrows C_2O_4^- \cdot (CO_2)_4$ at $n = 6$ (“electronic isomerization”). We have studied the structures of isomers for small $(CO_2)_n^-$ clusters and their isomerization processes by ab initio calculations. Structural evolution of $(CO_2)_n^-$ has been investigated by mass spectrometry.

III-F-1 *Ab initio* Study of $CO_2^- \cdot CO_2 \rightleftarrows C_2O_4^-$ Isomerization

SAEKI, Morihisa; TSUKUDA, Tatsuya; NAGATA, Takashi[1]
([1]*Univ. Tokyo)*

[*Chem. Phys. Lett.* in press]

The potential energy surface relevant to the isomerization of $(CO_2)_2^-$ has been investigated by *ab initio* calculations including effects of electron correlation. The surface plotted against appropriate angle parameters shows two shallow minima and a deep valley, which correspond to $CO_2^-\cdot CO_2$ (C_{2v}), $CO_2^-\cdot CO_2$ (C_s) and $C_2O_4^-$ (D_{2d}) structures, respectively. The transition states for the $C_{2v} \rightleftarrows C_s \rightleftarrows D_{2d}$ interconversion are located well below the CO_2^- + CO_2 dissociation limit, which allows $(CO_2)_2^-$ with sufficient internal energies to fluctuate among the isomeric forms. The calculations have also revealed quantitatively the behavior of the excess charge flow during the $CO_2^-\cdot CO_2 \rightleftarrows C_2O_4^-$ electronic isomerization.

Reference

1) M. Saeki, T. Tsukuda, S. Iwata and T. Nagata, *J. Chem. Phys.* **111**, 6333 (1999).

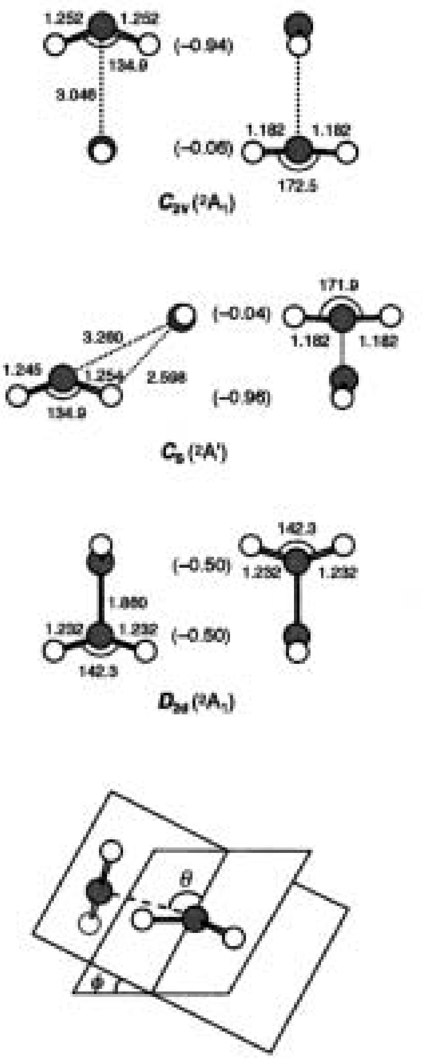

Figure 1. Top and side views of the geometries of $(CO_2)_2^-$ isomers optimized at the MP2/6-31+G* level (taken from reference 1). The digits in parentheses represent the Mulliken gross populations on the CO_2 moieties. Bond lengths and bond angles are given in Å and degrees. Also given in the figure are definitions of angle parameters θ and ϕ to describe the intermolecular motion during isomerization.

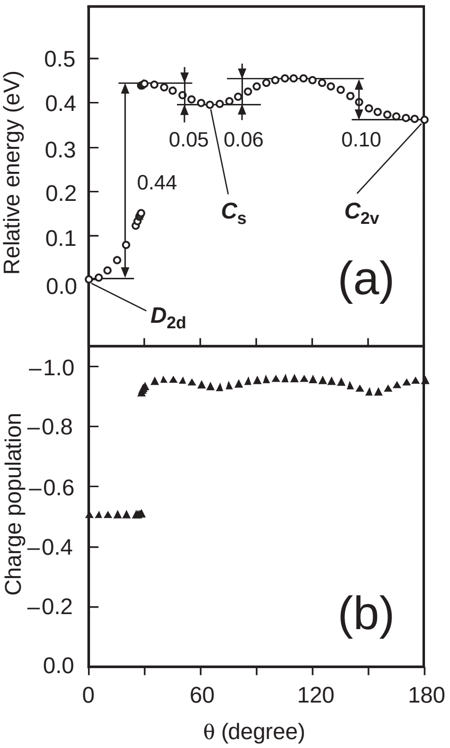

Figure 2. Potential profile along the minimum-energy path for the $(CO_2)_2^-$ isomerization (panel a) and the charge population at each transient structure (panel b) plotted against angle θ. The numbers in the panel (a) represent the barrier heights for the isomerization in electron volts. The charge population corresponds to the Mulliken gross populations on the CO_2 unit carrying a larger excess charge.

III-F-2 *Ab initio* Study of $(CO_2)_n^-$: Structures and Stabilities of Isomers

SAEKI, Morihisa; TSUKUDA, Tatsuya; NAGATA, Takashi[1]
([1]Univ. Tokyo)

[*Chem. Phys. Lett.* **340**, 376 (2001)]

The geometrical structures and stabilities of $(CO_2)_n^-$ with the size range $3 \le n \le 6$ are investigated by *ab initio* calculations including effects of electron correlation. The calculations have shown that the structures of $(CO_2)_n^-$ can be formulated by either $CO_2^-\cdot(CO_2)_{n-1}$ or $C_2O_4^-\cdot(CO_2)_{n-2}$, and that the geometry of $(CO_2)_2^-$ dimer remains more or less in all the optimized structures. In all the sizes investigated in the present study, the most stable isomers are of the $C_2O_4^-\cdot(CO_2)_{n-2}$ form, being consistent with the results obtained in the photoelectron spectroscopic studies.[1)]

Reference

1) T. Tsukuda, M. A. Johnson and T. Nagata, *Chem. Phys. Lett.* **268**, 429 (1997).

III-F-3 Structural Evolution of Large $(CO_2)_n^-$ Clusters as Studied by Mass Spectrometry

NEGISHI, Yuichi; NAGATA, Takashi[1]; TSUKUDA, Tatsuya

(*^{1}Univ. Tokyo)*

Negatively-charged clusters of CO_2 are generated by electron-impact ionized free jet expansion and analyzed by mass spectrometry. Figure 1 shows typical mass spectra of $(CO_2)_n^-$ covering the size range up to n ~ 1000 (m/z ~ 44000). Abrupt intensity drops in otherwise smooth distributions are observed in the size range of $n \le 150$, whereas a series of humps are discernible in the spectra recorded in the mass range $n \ge 150$. Weak but distinct intensity anomalies are also observed in the distributions of the $(CO_2)_n^+$ cluster cations in the size range of $n \le 150$, while oscillatory structures similar to those of $(CO_2)_n^-$ are observed in the $n \ge 150$ range. These comparisons suggest that the magic numbers associated with the small $(CO_2)_n^-$ clusters ($n \le 150$) reflect intrinsic stabilities of ions, and that the intensity distributions of larger $(CO_2)_n^-$ cluster are mostly determined by the abundance of neutral CO_2 clusters. To find reasonable structural models for $(CO_2)_n^-$, the magic numbers are compared with the sizes predicted from the Mackay icosahedral packing sequence. For $n \le 150$, the magic numbers observed experimentally (n = 14, 52, and 146) are close to the sizes predicted for icosahedral structures having complete layers (n = 13, 55, 147). These similarities suggest icosahedron-like structures for small $(CO_2)_n^-$ clusters which are somewhat deformed due to the presence of anionic cores. In contrast, the distributions for larger clusters cannot be explained by icosahedral structure model, being consistent rather with the cubic structures for neutral clusters in the $n \gg 55$ range.$^{1)}$

Reference

1) J.-B. Maillet, A. Boutin and A. H. Fuchs, *J. Chem. Phys.* **111**, 2095 (1999).

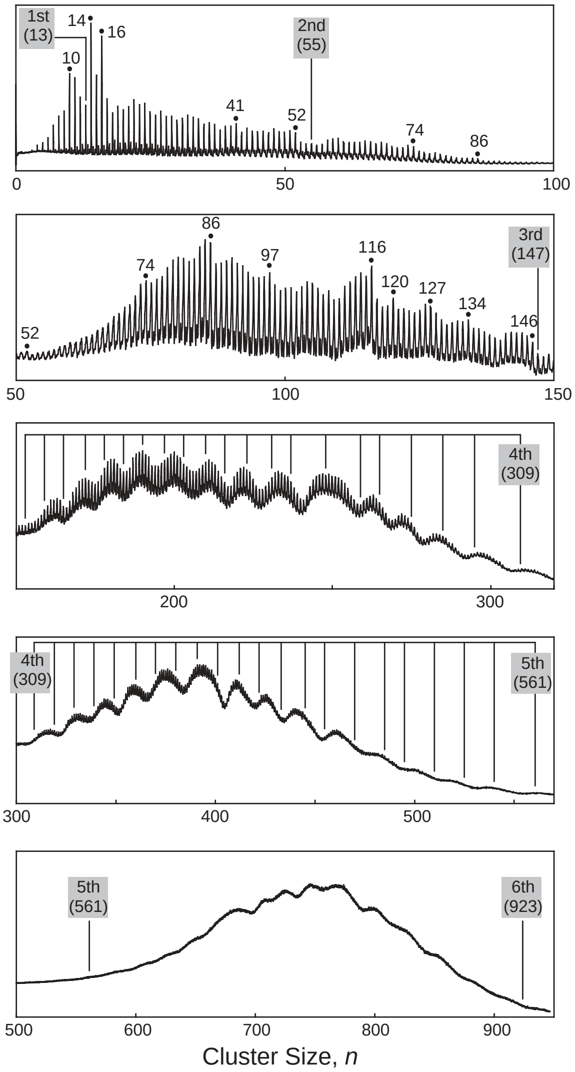

Figure 1. Typical mass spectra of $(CO_2)_n^-$. Bars in the figure represent the cluster sizes at which additional subshell structures are closed around the complete icosahedron structures. Note that these mass spectra are recorded while changing the deflection voltage so that the cluster ions of a given size range can be detected simultaneously.